Novel Epac fluorescent ligand reveals distinct Epac1 vs. Epac2 distribution and function in cardiomyocytes

Laëtitia Pereira[a], Holger Rehmann[b], Dieu Hung Lao[c], Jeffrey R. Erickson[a,d], Julie Bossuyt[a], Ju Chen[c], and Donald M. Bers[a,1]

[a]Department of Pharmacology, University of California, Davis, CA 95616; [b]Molecular Cancer Research, University Medical Center Utrecht, NL-3584 Utrecht, The Netherlands; [c]Department of Medicine, University of California, San Diego, La Jolla, CA 92093-0612; and [d]Department of Physiology, University of Otago, Dunedin, New Zealand 9013

Edited by John D. Scott, Howard Hughes Medical Institute, Department of Pharmacology, University of Washington School of Medicine, Seattle, WA, and accepted by the Editorial Board February 20, 2015 (received for review August 27, 2014)

Exchange proteins directly activated by cAMP (Epac1 and Epac2) have been recently recognized as key players in β-adrenergic–dependent cardiac arrhythmias. Whereas Epac1 overexpression can lead to cardiac hypertrophy and Epac2 activation can be arrhythmogenic, it is unknown whether distinct subcellular distribution of Epac1 vs. Epac2 contributes to differential functional effects. Here, we characterized and used a novel fluorescent cAMP derivate Epac ligand 8-[Pharos-575]-2′-O-methyladenosine-3′,5′-cyclic monophosphate (Φ-O-Me-cAMP) in mice lacking either one or both isoforms (Epac1-KO, Epac2-KO, or double knockout, DKO) to assess isoform localization and function. Fluorescence of Φ-O-Me-cAMP was enhanced by binding to Epac. Unlike several Epac-specific antibodies tested, Φ-O-Me-cAMP exhibited dramatically reduced signals in DKO myocytes. In WT, the apparent binding affinity (K_d = 10.2 ± 0.8 μM) is comparable to that of cAMP and nonfluorescent Epac-selective agonist 8-(4-chlorophenylthio)-2-*O*-methyladenosine-3′-,5′-cyclicmonophosphate (OMe-CPT). Φ-O-Me-cAMP readily entered intact myocytes, but did not activate PKA and its binding was competitively inhibited by OMe-CPT, confirming its Epac specificity. Φ-O-Me-cAMP is a weak partial agonist for purified Epac, but functioned as an antagonist for four Epac signaling pathways in myocytes. Epac2 and Epac1 were differentially concentrated along T tubules and around the nucleus, respectively. Epac1-KO abolished OMe-CPT–induced nuclear CaMKII activation and export of transcriptional regulator histone deacetylase 5. In conclusion, Epac1 is localized and functionally involved in nuclear signaling, whereas Epac2 is located at the T tubules and regulates arrhythmogenic sarcoplasmic reticulum Ca leak.

cardiomyocytes | Epac1 | Epac2 | localization | fluorescence

Cyclic adenosine 3′,5′-monophosphate (cAMP) is a prominent multifunctional intracellular second messenger (1). In heart, elevation of cAMP, upon sympathetic stimulation of β-adrenergic receptors (β-AR) controls cardiac function via regulation of processes such as electrophysiology, excitation–contraction (EC) coupling, and gene expression. In heart failure, chronic β-AR stimulation contributes to arrhythmias and cardiac remodeling. Until recently, cAMP downstream effects were mostly attributed to PKA. However, cAMP also stimulates exchange protein directly activated by cAMP (Epac) (2, 3) and recent studies in cardiac myocytes (4–14) have demonstrated that Epac can mediate cAMP-dependent effects (independently of PKA), including altered EC coupling, arrhythmias, and transcriptional regulation.

There are two main Epac isoforms, Epac1 and Epac2, encoded by two independent genes, Rap guanine nucleotide exchange factor (RAPGEF) 3 and 4. Epac1 and Epac2 share high structural homology with comparable dishevelled, Egl-10, and pleckstrin (DEP), Ras exchange motif (REM), guanine exchange factor (GEF) and cAMP-binding domains (cNBDs) (15). Epac1 contains one cAMP-binding domain (cNBD-B), whereas Epac2 has two (cNBD-A and cNBD-B). Differences between Epac1 and Epac2 may dictate distinct subcellular localization and function. Indeed, in MIN6-insulin secreting cells, cNBD-A was required for targeting Epac2 near the plasma membrane (16) and in PC12 cells, the Epac1 catalytic region was suggested to be responsible for nuclear targeting (17). In other cell lines Epac1-based cAMP FRET sensors or expressed Epac1 tagged with GFP (Ad-Epac1-GFP) expressed at the cytosol, plasma membrane, and mitochondria (16–22), and moved to the plasma membrane upon activation (23). In adult cardiomyocytes, subcellular localization and function of endogenous Epac1 and Epac2 are not yet clear.

In neonatal and adult cardiomyocytes, Ad-Epac1-GFP expresses at T tubules, cytosol, and nuclear membrane (6, 7). Epac1 localization at perinuclear membranes of hypertrophic neonatal cardiomyocytes suggests its role in maladaptive hypertrophy (24, 25). Consistent with that, Epac1 mRNA is up-regulated in human heart failure and animal models of hypertrophy (induced by pressure overload or catecholamines). Epac1 also seems to be part of a nuclear mAKAP/PKA/PDE4/ErK5 complex to regulate cAMP signaling (24). Indeed, Epac activation by adenoviral Epac1 expression or the specific Epac agonist 8-(4-chlorophenylthio)-2-*O*-methyladenosine-3-,5-cyclic monophosphate (OMe-CPT), can activate hypertrophic transcription regulators MEF2 and NFAT, via phospholipase C (PLC)/IP_3/Ca/Ca-calmodulin kinase II (CaMKII)/HDAC4-HDAC5 (5, 11) and H-Ras/Ca/calcineurin pathways (6, 7), respectively. Epac activation in myocytes influences both nuclear and cytosolic Ca signaling modifying transcription and EC coupling and arrhythmias. For example, sustained Epac activation increases expression of calmodulin, leading to Ca mishandling and

Significance

β-Adrenergic activation in heart has many important effects (physiological and pathological) that had been mainly attributed to cAMP and protein kinase A-dependent signaling. The discovery of exchange protein directly activated by cAMP (Epac1 and Epac2) has uncovered new parallel cAMP signaling pathways in β-adrenergic signaling, but Epac isoform localization and function were not well understood. Here we show, using a novel fluorescent Epac analog, that Epac1 and Epac2 are differentially concentrated at the nucleus vs. at Z lines in cardiomyocytes, and that this corresponds to functional roles in nucleus vs. calcium handling and arrhythmias, respectively. This finding may be essential to develop more targeted therapeutics for cardiomyopathy.

Author contributions: L.P. and D.M.B. designed research; L.P., H.R., and J.R.E. performed research; D.H.L., J.B., and J.C. contributed new reagents/analytic tools; L.P. and H.R. analyzed data; and L.P. and D.M.B. wrote the paper.

The authors declare no conflict of interest.

This article is a PNAS Direct Submission. J.D.S. is a guest editor invited by the Editorial Board.

[1]To whom correspondence should be addressed. Email: dmbers@ucdavis.edu.

This article contains supporting information online at www.pnas.org/lookup/suppl/doi:10.1073/pnas.1416163112/-/DCSupplemental.

CELL BIOLOGY

enhancing susceptibility to arrhythmia (12). Epac-dependent arrhythmia is also observed during acute Epac activation through CaMKII-dependent activation of diastolic Ca leak from the sarcoplasmic reticulum (SR) due to ryanodine receptor (RyR) phosphorylation and involving PLC, Rap, and IP_3 receptors (4, 8–10). We recently showed that activation of Epac2, but not Epac1, induces β1-AR–induced arrhythmias through CaMKII-dependent diastolic SR Ca release (14). We hypothesize that cardiac Epac1 and Epac2 mediate different functions, in part because of distinct subcellular localization. However, available Epac antibodies may lack specificity in immunolocalization studies, rendering information on Epac isoform localization equivocal.

Here, we characterize a novel commercially available fluorescent Epac ligand that has not been previously described, 8-[Pharos-575]-2′-O-methyladenosine-3′,5′-cyclic monophosphate (Φ-O-Me-cAMP). We characterized and used it to clarify Epac isoform localization in adult ventricular myocytes, in mice in which one or both Epac isoforms were knocked out [Epac1-KO, Epac2-KO, and double knockout (DKO) mice] (14). We found that Epac2 is highly concentrated at Z lines in cardiomyocytes, consistent with our study implicating Epac2 selectivity in SR Ca-dependent arrhythmogenesis. In contrast, Epac1 was more concentrated at the nuclear envelope. This is consistent with our findings here that Epac-dependent nuclear export of histone deacetylase 5 (HDAC5) is abolished in Epac1-KO mice and mediated by β1-AR. Thus, differential localization of Epac isoforms strongly influences their functional roles in cardiac myocytes.

Results

Spectral Characteristic of Φ-O-Me-cAMP. Φ-O-Me-cAMP is a fluorescent cAMP analog with a 2′-O-methyl substitution on the ribose ring, providing specificity (as in OMe-CPT) for Epac vs. PKA (26) (Fig. 1*A*). Φ-O-Me-cAMP differs from OMe-CPT by the substitution of the 8-(4-chlorophenylthio) group by the fluorescent Pharos group (Fig. 1*A*), which could alter Epac vs. PKA selectivity (27, 28). Free Pharos fluorescence has excitation and emission peaks at 575 and 617 nm, respectively (29). Emission and excitation scans for Φ-O-Me-cAMP (Fig. 1 *B* and *C*) show slight spectral shifts vs. Pharos, but are similar to [Pharos-575]-cAMP, a nonmethylated cAMP agonist lacking Epac selectivity (29). Φ-O-Me-cAMP (10 μM) emission intensity is increased when Epac is present (Fig. 1*C* and Fig. S1). For myocyte studies we used 534 nm excitation, the wavelength at which Φ-O-Me-cAMP fluorescence was most strongly enhanced by cell lysate protein (A/B is near 3 for 10 μM Φ-O-Me-cAMP; Fig. 1*C*, *Inset*).

Φ-O-Me-cAMP Binding and Effects on Nucleotide Exchange. We used purified proteins to measure Epac-dependent nucleotide (GDP) exchange on Rap1, a known proximal Epac effector. Φ-O-Me-cAMP partially activated Epac1, but only at concentrations above 10 μM, and to much lower activity than for 100 μM cAMP (Fig. 1*D*). When both ligands were combined (at 100 μM), Φ-O-Me-cAMP suppressed Epac1 activity vs. cAMP alone, consistent with a weak partial agonist effect of Φ-O-Me-cAMP on Epac1 (Fig. 1*E*). For Epac2, 100 μM Φ-O-Me-cAMP produced negligible activation, but could limit activation by cAMP (Fig. 1*E*). The degree to which equimolar Φ-O-Me-cAMP inhibits cAMP-induced Epac activity suggests that Φ-O-Me-cAMP has a slightly lower Epac affinity vs. cAMP.

To test for Φ-O-Me-cAMP binding to Epac in cells, intact cardiac myocytes were exposed to Φ-O-Me-cAMP in physiological solution (Fig. 2*A*). Φ-O-Me-cAMP binding was saturable, with an apparent K_d = 10.2 ± 0.8 μM (Fig. 2 *A* and *B*), which is between values reported for cAMP (K_d = 30–45 μM for Epac 1) and OMe-CPT (K_d = 2 μM) (26–28, 30). In myocytes lacking Epac (DKO), a low level of binding was observed [~25% of wild type (WT)] with an apparent K_d of 3.4 ± 0.4 μM (Fig. 2 *A* and *B*).

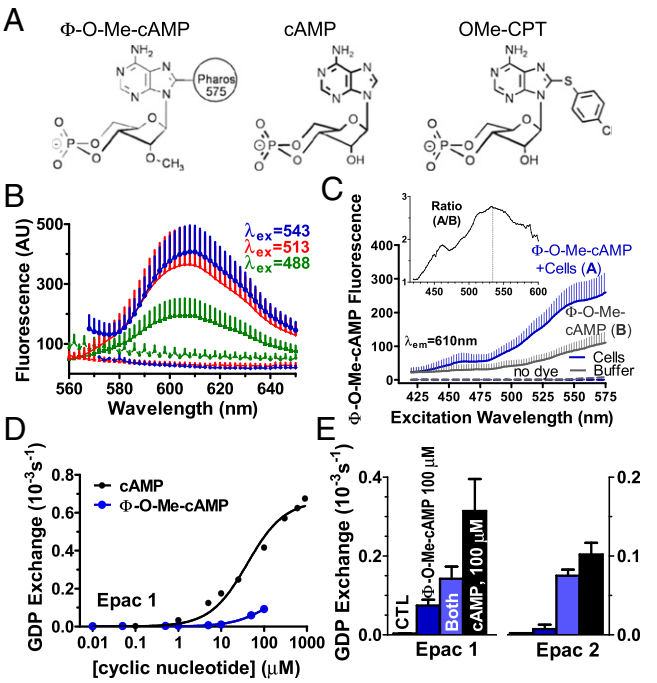

Fig. 1. Spectral analysis of Epac ligand, Φ-O-Me-cAMP. (*A*) Structure of Φ-O-Me-cAMP, cAMP, and Epac selective activator (OMe-CPT). (*B*) Cell emission spectra with (top) and without (bottom) Φ-O-Me-cAMP for indicated λ_{ex}. (*C*) Excitation spectra for λ_{em} = 610 nm in cell lysate (blue) vs. buffer (gray) with (solid) or without (dashed) 10 μM Φ-O-Me-cAMP. (*Inset*) Ratio of curves A/B, after background subtraction ($n \geq 3$). (*D*) Purified Epac1-mediated GDP exchange rate constant on Rap1b at different [cAMP] and [Φ-O-Me-cAMP]. (*E*) Epac GDP exchange activity toward Rap1b in presence of indicated cyclic nucleotides (100 μM).

Thus, most Φ-O-Me-cAMP binding in myocytes is due to Epac, but it also binds specifically to a non-Epac target in the myocyte (conceivably a phosphodiesterase). Correcting for this non-Epac component reduces the B_{max} and apparent Epac affinity, so those values are approximations. Φ-O-Me-cAMP is lipophilic (29) and Fig. 2*C* shows the time course of Φ-O-Me-cAMP binding in intact cardiomyocytes and suppression by OMe-CPT. Maximal Φ-O-Me-cAMP binding was reached at 30 min (Fig. 2*C*) and washed out with a $\tau_{washout}$ of 6.5 min (Fig. 2*D*).

Φ-O-Me-cAMP Specificity for Epac and Epac Function in Myocytes. Fig. 3*A* shows confocal images of Φ-O-Me-cAMP in intact mouse from WT and DKO cardiac myocytes (14). Φ-O-Me-cAMP binding was reduced by ~75% in DKO and also by pretreatment with 100 μM of the Epac agonist OMe-CPT (Fig. 3 *A* and *B*). However, as in intact cells, a non-Epac residual signal was seen. Fig. 3*C* shows the time course of wash-in and -out of 1 μM Φ-O-Me-cAMP in saponin-permeabilized myocytes. OMe-CPT again depressed the signal substantially. The stability of the plateau phase and level of binding (vs. intact myocytes) suggests that Epac itself does not quickly wash out of permeabilized cardiac myocytes. At 1 μM Φ-O-Me-cAMP fluorescence was small in the absence of cells (Fig. 3*C*). To test whether Φ-O-Me-cAMP could activate PKA target phosphorylation, we used an adenoviral PKA-based FRET biosensor, AKAR (Fig. 3*D*). Isoproterenol (ISO) enhanced AKAR FRET, providing a positive control. Neither 10 μM Φ-O-Me-cAMP nor 10–100 μM OMe-CPT activated PKA activity (Fig. 3*D*) confirming Φ-O-Me-cAMP selectivity for Epac vs. PKA in cardiac myocytes.

The Epac-based cAMP-FRET biosensor (ICUE1) (Fig. S2) incorporates full-length Epac1, and FRET efficiency can be measured by enhanced donor (CFP) fluorescence upon acceptor (YFP)

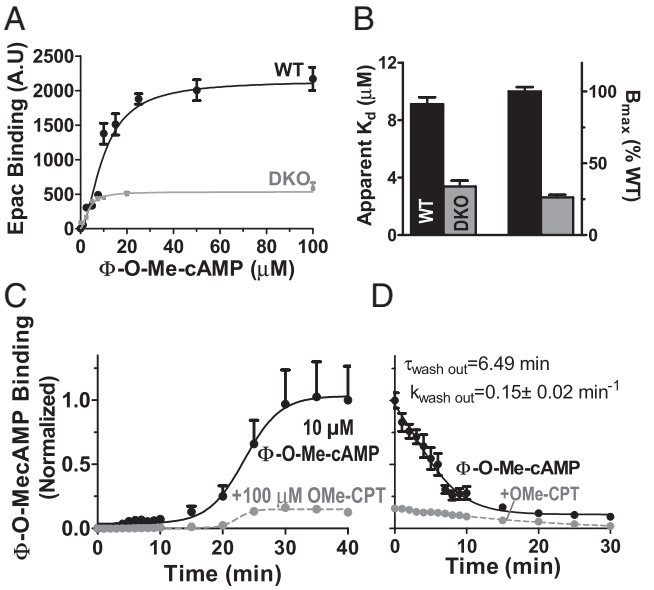

Fig. 2. Φ-O-Me-cAMP binding in intact cardiac myocytes. (*A*) Φ-O-Me-cAMP binding (as fluorescence intensity) as function of [Φ-O-Me-cAMP] in intact WT and DKO myocytes (cell numbers are n = 9–26 for WT and n = 4–39 for DKO). (*B*) Apparent K_d and B_{max} from fits of data from *A* to $y = B_{max}/(1 + (K_d/x)^{1.74})$. Mean 10 μM Φ-O-Me-cAMP binding during wash-in (*C*) and wash-out (*D*), ±OMe-CPT in intact WT cardiomyocytes (n = 13 vs. n = 17 and n = 8 vs. n = 10).

photobleach (Fig. 4 *A* and *B*). Both Φ-O-Me-cAMP and OMe-CPT (at 10 μM) reduced FRET in ICUE1 (Fig. 4*C*), confirming that they both bind to the cAMP domain of Epac1 and cause conformational changes.

ISO and OMe-CPT can induce ICUE1 translocation to the plasma membrane in HEK293 cells (18, 23). We see this also in cardiac myocytes for treatment with ISO, OMe-CPT, and ISO + PKA inhibition, but that effect is blocked by pretreatment with Φ-O-Me-cAMP (Fig. S3). We also detect OMe-CPT–induced nuclear export of Epac1-YFP in myocytes (Fig. 4*D*). This was not replicated by Φ-O-Me-cAMP and was prevented by Φ-O-Me-cAMP. OMe-CPT also induces a robust increase in Ca spark frequency in myocytes, which we have shown requires Epac2 (14). That effect is blocked by Φ-O-Me-cAMP, which by itself did not activate Ca sparks (Fig. 4*E*). Epac activation by O-Me-CPT induces nuclear export of the transcriptional regulator HDAC5 (11), which was blocked and not mimicked by Φ-O-Me-cAMP (Fig. 4*F*). Thus, for all four of these known downstream Epac functional effects in cardiac myocytes (5, 11, 21, 23), Φ-O-Me-cAMP behaves like an antagonist (i.e., partial agonist effects were not apparent).

Cardiac Epac1 and Epac2 Localization. Our preliminary immunohistochemistry studies to assess Epac isoform localization in cardiac myocytes were unsuccessful, due to antibody limitations (i.e., relatively similar signals of Epac1 antibodies in DKO vs. WT mice; Fig. S4). We used 10 μM Φ-O-Me-cAMP in Epac1 and Epac2-KO cardiomyocytes to assess endogenous Epac1 and Epac2 distribution. Cardiomyocytes were loaded with Φ-O-Me-cAMP together with the voltage-sensitive dye di-8ANEPPS (to assess T tubules; Fig. 5*A*) or MitoTracker Green (to assess mitochondria; Fig. 5*C*). These compartments had been reported as sites of Ad-Epac1 or Epac1 FRET sensors expression in cells (16–22). Fluorescence cross-talk was negligible for these colocalization studies (Fig. S5). Φ-O-Me-cAMP B_{max} signals (as in Fig. 2 *A* and *B*) for WT, Epac1-KO, Epac2-KO, and DKO myocytes imply that in WT myocytes, roughly half of Φ-O-Me-cAMP is bound to Epac2 and 25% each to Epac1 and non-Epac site (Fig. S6).

Φ-O-Me-cAMP fluorescence in Epac1-KO mice (i.e., Epac2 location) was similar to the striated signal from di-8-ANEPPS, with peak intervals near 1.8 μm characteristic of T tubules [Φ-O-Me-cAMP: 1.75 ± 0.02 μm, n = 11 vs. di-8-ANEPPS 1.75 ± 0.02, n = 11; P = not significant (N.S.)] (Fig. 5*B*). Similar widths at half maximum peak (full width at half maximum, FWHM) suggest a similarly narrow spatial focus for both (Fig. 5*B*). This result agrees with our previous functional findings that Epac2 is sufficient to fully recapitulate the Epac-mediated activation of SR Ca leak (14), because the RyR2 release sites are mainly along the T tubules. In contrast, Epac1 (in Epac2-KO cells) did not show sarcomeric striations (Fig. 5*D*), but showed concentration at the nuclear envelope, compared with either WT or Epac1-KO myocytes (Fig. 5 *E* and *F*). For WT and Epac2-KO there is clear enhancement of Epac at the nuclear edge compared with the nuclear interior [shown as nuclear envelope (NE) to nuclear ratio]. In contrast, when only Epac2 is present, fluorescence was low throughout the nucleus and NE, rising only when it reaches the sarcomeric Epac2 location outside that NE region. We did not detect Epac1 to be highly concentrated at either the sarcolemma or mitochondria.

Epac1 Is at the Nucleus to Regulate Transcriptional Pathways. In both adult and neonatal cardiomyocytes, Epac1 overexpression mediates β-AR–dependent hypertrophic signaling and activation of gene transcription via CaMKII/HDAC5/MEF2 and calcineurin/NFAT pathways (5, 11). In isolated cardiac myocytes, we used the FRET sensor Camui (full-length CaMKII flanked by CFP and YFP at the N and C termini) where FRET is maximal in the basal autoinhibited state (31). Epac stimulation by OMe-CPT activated CaMKII (Fig. 6 *A* and *B*), nearly as well as ISO in our previous study (31). However, this effect was abolished in a mutant Camui lacking the T286 autophosphorylation site (T286A), suggesting that

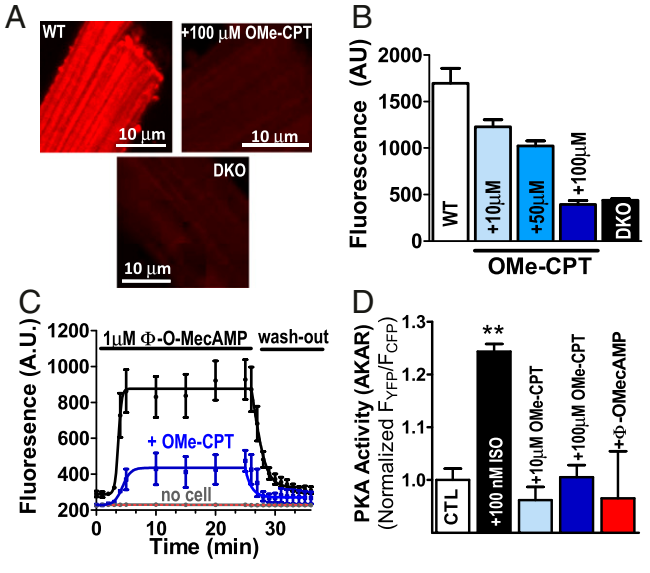

Fig. 3. Φ-O-Me-cAMP specificity for Epac in myocytes. (*A*) Confocal images of Φ-O-Me-cAMP binding in WT (±100 μM OMe-CPT) and Epac1/2 double knockout mice (DKO). (*B*) Φ-O-Me-cAMP binding in intact WT myocytes (n = 13) decreased with increasing [OMe-CPT] (n = 16, 28, and 20) and in DKO (n = 52). (*C*) Epac binding of Φ-O-Me-cAMP in permeabilized WT myocytes ± OMe-CPT (n = 6–7) and with no cells (gray) and without cells or Φ-O-Me-cAMP (red). (*D*) PKA activity assessed with Ad-AKAR FRET-based sensor under isoproterenol (ISO, 100 nM; n = 40), OMe-CPT (10 μM, n = 20; 100 μM, n = 20), and Φ-O-Me-cAMP (n = 12) vs. WT (n = 50). **P < 0.01 vs. control (CTL).

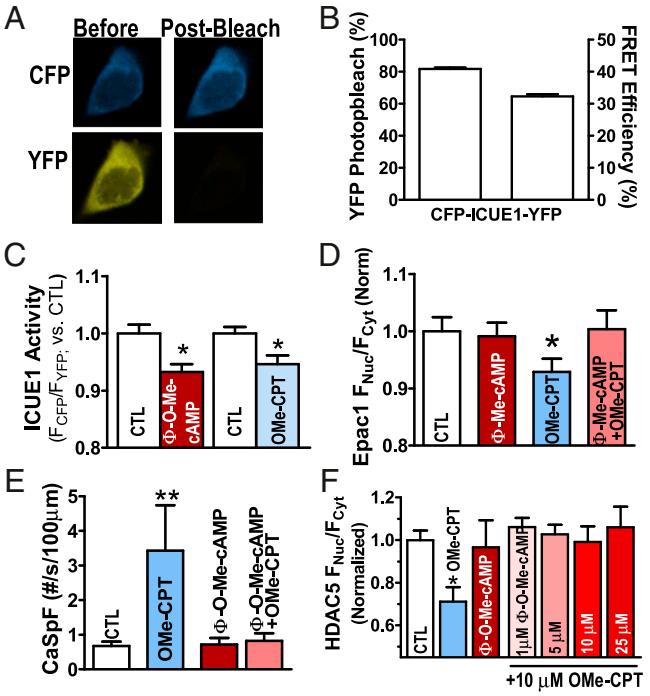

Fig. 4. Φ-O-Me-cAMP binds Epac, without activation. (*A*) CFP signal increase after YFP photobleach in HEK293 cells. (*B*) Extent of YFP photobleach (n = 75) and baseline FRET efficiency of CFP-ICUE1-YFP (n = 85). (*C*) Mean ICUE1 signal at baseline (n = 45 and 87), upon 10 μM OMe-CPT (n = 58), or 10 μM Φ-O-Me-cAMP (n = 91) in HEK293 cells after 30-min incubation. (*D*) Epac1-YFP translocation in cultured cardiomyocytes from WT at baseline (n = 27), with Φ-O-Me-cAMP ± OMe-CPT (n = 31 and n = 17) and with OMe-CPT alone (n = 27). (*E*) Ca spark frequency (CaSpF) in myocyte under the same treatments (n = 18, n = 13, n = 13, and n = 7, respectively). (*F*) HDAC5-GFP translocation in cultured myocytes from WT at baseline (n = 64), with OMe-CPT (n = 19), and plus increasing [Φ-O-Me-cAMP] (n = 13, 10, 8, 9, 10). *P < 0.05 vs. CTL.

Epac-dependent activation requires CaMKII autophosphorylation (Fig. 6 *A* and *B*). Because cytosolic CaMKII (and Camui) is concentrated along the T tubules (like Epac2), this cytosolic CaMKII activation is dominated by Epac2 activation, as previously described (14).

Nuclear CaMKII activity was also significantly increased by OMe-CPT exposure (increased F_{CFP}/F_{YFP}; $P < 0.001$; Fig. 6*C*) and was abolished by 2-APB [an inositol-1,4,5-trisphosphate (IP_3) inhibitor]. This is consistent with nuclear IP_3 receptor-dependent activation of nuclear CaMKII (32). Nuclear CaMKII activation also requires autophosphorylation (Fig. 6*C*). Previous work showed that OMe-CPT–induced HDAC5 nuclear export was entirely CaMKII and IP_3 receptor dependent (5, 11). Consistent with this, we found that HDAC5 nuclear export was blocked by CaMKII inhibitor KN-93 and by 2-APB (Fig. 6*D*). We also find here that the OMe-CPT–induced nuclear export of HDAC5 was completely prevented in Epac1-KO mice (Fig. 6*D*), consistent with perinuclear Epac1 vs. Epac2. Both Epac and HDAC5 translocation were also prevented by β1-AR block by CGP20712A (Fig. 6 *E* and *F*). Altogether, these results suggest that Epac1 is sufficient (in part because of its localization) in nuclear signaling via the IP_3/CaMKII/HDAC5 transcriptional regulation pathway and that this pathway is selectively mediated by Epac1 and β1-AR stimulation.

Discussion

Epac2 was recently identified as the isoform responsible for Epac-mediated SR Ca leak and arrhythmia (14), suggesting isoform-specific signaling pathways. However, Epac1 and Epac2 localization in cardiac myocytes, critical for clarifying Epac function in cardiac pathologies such as hypertrophy and arrhythmia, were not clear. Here, we provide evidence, using a novel fluorescent Epac ligand Φ-O-Me-cAMP, that Epac1 and Epac2 are compartmentalized. The permeability, specificity, and binding affinity of Φ-O-Me-cAMP make it a useful tool to define endogenous Epac1 and Epac2 distribution in cardiomyocytes. We found that endogenous Epac2 is concentrated in T tubules, facilitating its ability to influence CaMKII-dependent RyR phosphorylation and raise SR Ca leak to trigger arrhythmias. In contrast, endogenous Epac1 was most clearly concentrated in the perinuclear region, positioned well to regulate nuclear signaling and β1-AR–mediated gene transcription involved in cardiac hypertrophy.

Φ-O-Me-cAMP, a Novel Epac Fluorescent Indicator. Until now, nonfluorescent tools have helped clarify the biological roles of Epac vs. PKA (26, 33, 34). Φ-O-Me-cAMP is a novel fluorescent Epac ligand, which we find to be a partial agonist, but at concentrations used in myocytes here (≤10 μM), it acts mainly as a competitive antagonist on Epac signaling, as it blocks all OMe-CPT–mediated effects studied. As in OMe-CPT, this fluorescent cAMP analog has specificity for Epac over PKA. The Pharos vs. pCPT group results in somewhat lower Epac affinity vs. OMe-CPT (26–28, 30), which agrees with the pCPT group's importance for

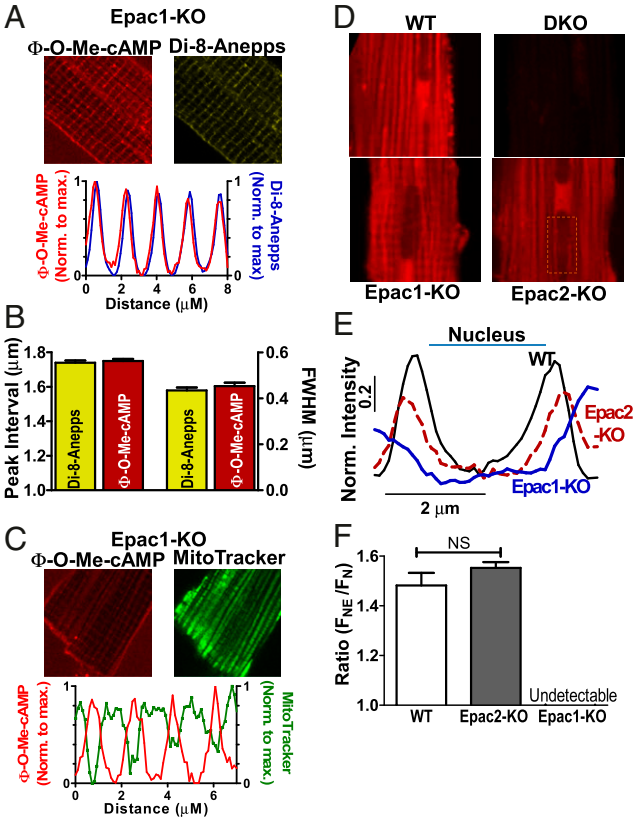

Fig. 5. Epac2 located at T tubules vs. Epac1 at nuclear membrane. (*A*) Colocalization in Epac1-KO myocytes (showing Epac2) loaded with Φ-O-Me-cAMP and membrane dye (di-8-ANEPPS, n = 16) and fluorescence profile. (*B*) Mean of peak interval and full width at half maximum of peak (FWHM) for data as in *A*. (*C*) Alternating distribution of Epac2 and mitochondria (using MitoTracker) in Epac1-KO myocytes. (*D*) Confocal images of Φ-O-Me-cAMP loading in WT, Epac1-KO, Epac2-KO, and DKO cardiomyocytes with their respective profiles at the nuclear region (*E*). (*F*) Average of ratio of nuclear envelope (F_{NE}) over inside nucleus signal (F_N) ratio for each groups. WT (n = 11), Epac1-KO (n = 13), and Epac2-KO (n = 15). P = N.S.

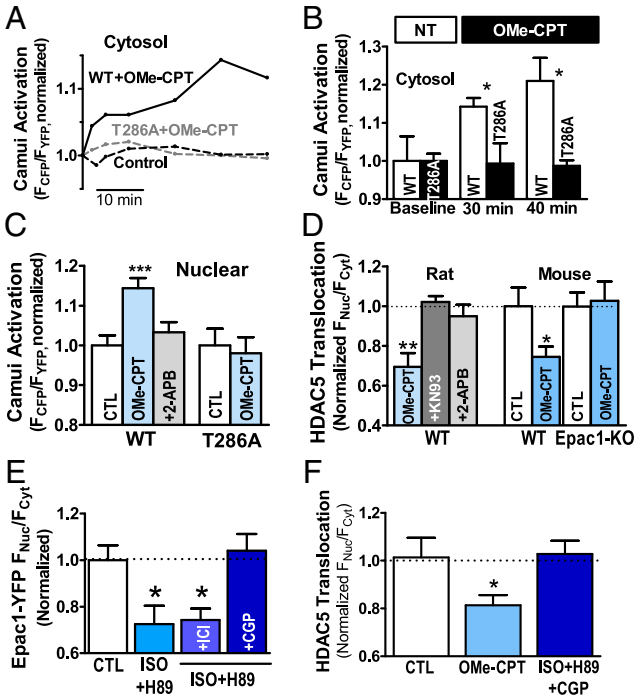

Fig. 6. Epac1 mediates CaMKII-dependent HDAC5 nuclear export. (*A*) CaMKII FRET-based activity reporter Camui signals for WT and nonphosphorylable mutant (T286A) Camui in rat myocytes. (*B*) Mean values for data as in *A* (10 μM OMe-CPT, Camui-WT (n = 22 and 16), and Camui-T286A (n = 13 and 24) vs. baseline (n = 17 for Camui-WT and n = 26 for Camui-T286A). (*C*) Activation of nuclear Camui-WT ± OMe-CPT (n = 16 vs. n = 11) or 2-APB (n = 7) and Camui-T286A ± 8-pCPT (n = 25 vs. n = 11). (*D*) Mean of HDAC5-GFP translocation in WT rat with OMe-CPT ± CaMKII inhibitor (KN93, n = 10) or IP_3-R blocker (2-APB, n = 9) as well as in WT mouse (n = 16 and n = 19) and Epac1-KO mice ± OMe-CPT (n = 16 and n = 13). (*E*) Epac1-YFP and HDAC5-GFP (*F*) translocation in presence of either β1-AR block (CGP; n = 29 and n = 30) and β2-AR block (ICI; n = 6) compared with CTL baseline (n = 19 and n = 16) and OMe-CPT (n = 19) or ISO + H89 (n = 7). *P < 0.05, **P < 0.01, ***P < 0.001.

OMe-CPT affinity (33). Φ-O-Me-cAMP excitation in the visible range is advantageous vs. fluorescent nucleotides that require UV excitation, which can harm cells.

Φ-O-Me-cAMP, a Fluorescent Tool for Epac Localization. Epac1 and Epac2 share high homology, and the Epac1 antibodies we tested were not suitable for immunolocalization because of strong signals observed in the total absence of Epac (DKO). In contrast, Φ-O-Me-cAMP signal was greatly reduced both in DKO myocytes and by competition with the Epac-selective agonist OMe-CPT, indicating the specificity that is key for a useful fluorescent probe (35). Despite homology between the Epac and PKA binding domains (36), we find no evidence for Φ-O-Me-cAMP binding to PKA. Moreover, neither OMe-CPT nor Φ-O-Me-cAMP, at the concentrations used, could activate PKA. We could detect a residual and saturable signal when Φ-O-Me-cAMP was used in the DKO (Fig. 3*A*). This signal seems not to be due to Φ-O-Me-cAMP degradation by PDE (29), but because many cAMP analogs bind to phosphodiesterase isoforms (37), that might explain the non-Epac binding.

In addition, Φ-O-Me-cAMP has the advantage of being membrane permeable, unlike most fluorescent nucleotides, presumably due to the highly lipophilic Pharos dye (29). Indeed, the hydrophobic 8 substitution on cAMP analogs enhances their membrane permeability (33). In our conditions, Φ-O-Me-cAMP reached maximal binding within 30 min. Functionally, Φ-O-Me-cAMP binds to Epac without activating HDAC5 translocation, Epac1 translocation, and Epac2-mediated SR Ca leak, suggesting that Φ-O-Me-cAMP binding does not activate Epac signaling to these downstream targets in myocytes. Moreover, Φ-O-Me-cAMP prevents OMe-CPT–dependent activation of these pathways. So, although Φ-O-Me-cAMP is a partial agonist (particularly on Epac1 GDP exchange), it behaves mainly as an Epac antagonist in cellular signaling. However, caution should be used in interpreting Φ-O-Me-cAMP inhibition effects on Epac, keeping in mind the partial agonist effect, especially for Epac1. Φ-O-Me-cAMP permeability, specificity, affinity, and functional effects make it an effective tool to study basal endogenous Epac distribution (and serve in some cases as a functional antagonist).

Epac2 Is Distributed at the T Tubule to Mediate Arrhythmia. Φ-O-Me-cAMP binding in Epac1-KO and Epac2-KO cardiomyocytes revealed isoform compartmentalization. Epac2 was concentrated in T tubules, whereas Epac1 was concentrated around the nucleus. Previous work suggested that Epac1 appeared at plasma membranes and mitochondria (17–23), and we cannot exclude that some Epac1 is at these sites. Some previous work used exogenous expression of Epac1 constructs, which could alter localization. In Epac1-KO, Epac2 was not detected around the nucleus but was especially concentrated in the T tubules, the site of RyR and Ca-induced Ca-release during EC coupling (38, 39). That finding is consistent with a regulatory role for Epac2 on RyR function during β-AR stimulation. Indeed, β1-AR stimulation activates Epac2-mediated SR Ca leak and triggers arrhythmia by CaMKII-dependent phosphorylation of RyR in cardiac myocytes and intact murine hearts (4, 8–10, 12, 14). This propensity for arrhythmias could also be exacerbated by an Epac-mediated down-regulation of slow delayed rectifier potassium channels (40, 41) mediated by Epac translocation, which could prolong action potential duration and increase arrhythmogenic risk.

Epac1, a Key Player in Gene Transcription. Our perinuclear Epac1 localization agrees with work showing that Epac1 is part of a nuclear complex with a PKA anchoring protein mAKAP in hypertrophied neonatal cardiomyocytes (24). Moreover, Epac1-KO fully prevented OMe-CPT–dependent HDAC5 translocation, consistent with its involvement in maladaptive hypertrophy. Indeed, Epac1 is up-regulated in human heart failure and animal models of hypertrophy (6, 13). Epac activation can also elevate nuclear Ca, activating CaN/NFAT and CaMKII/HDAC hypertrophic pathways. These signaling pathways seem to be mediated only by β1-AR (Fig. 6 *E* and *F*). Moreover, Epac induced activation of nuclear CaMKII and HDAC5 translocation (Fig. 6), which can alter gene transcription by derepression of MEF2. Under sustained activation, Epac enhanced nuclear Ca release by IP_3 receptors, leading to up-regulation of calmodulin, which may also influence arrhythmogenesis (11, 12). Epac1 may also be part of a complex with CaMKII and β-arrestin (42), where local activation and translocation of Epac1 could influence CaMKII activation elsewhere in the cell. Finally, our work excludes participation of Epac2 in HDAC5 dependent hypertrophy, because HDAC5 nuclear export was abolished by Epac1 deletion.

In conclusion, our work demonstrates the importance of Epac1 and Epac2 distribution in adult ventricular myocytes and how that contributes to distinct functional roles for each isoform. Epac2 localized at T tubules and can mediate cardiac arrhythmias, whereas Epac1 at the nuclear envelope can regulate β1-AR–mediated gene transcription. Our characterization of the novel Epac ligand Φ-O-Me-cAMP, instrumental here, should allow this tool to become more broadly useful for understanding Epac localization and signaling in other cell types. Our work also raises the possibility that Epac1 activation can mediate rather than be a consequence of cardiac hypertrophic remodeling, but will require further study. Thus, the two Epac isoforms may present functionally distinct therapeutic targets

to be explored in the treatment of cardiac hypertrophy and arrhythmia.

Methods

Additional methods are described in *SI Methods*. Myocyte isolation was performed in adult Wistar rats and Epac1-KO, Epac2-KO, DKO, and C57BL6 mice using retrograde Langendorff perfusion and type-2 collagenase (Worthington) (37 °C) as previously described (14). All procedures were approved by the University of California Davis Institutional Animal Care and Use Committee. Data were expressed as mean ± SEM. Significance was evaluated by using unpaired or paired Student's *t* test, or two-way ANOVA as appropriate.

Spectral analysis of Φ-O-Me-cAMP (Biolog) was performed using spectrofluorometer (MS SpectraMax; Molecular Devices). Isolated rat cardiomyocytes were lysed by sonication in 20 mM Hepes buffer (pH = 7.2) with a protease inhibitor mixture (Calbiochem). After centrifugation (805 × *g*, 2 min), debris-free myocyte lysate was removed and diluted. Spectra were measured from 420 to 580 nm (λ_{em} = 610 nm) with slits set at 2 nm. FRET efficiency of CFP-ICUE1-YFP sensor was determined by acceptor (YFP) photobleach (40 s) using confocal microscopy. Excitation was via Argon laser (458 nm; CFP) and 514 nm (YFP) with emission at 485 ± 15 nm (CFP) or at ≥535 nm (YFP). For colocalization studies myocytes were loaded with Φ-O-Me-cAMP (10 μM, 30 min) and di-8-ANEPPS or MitoTracker Green (200 nM; 45 min). Excitation was at 450 nm for di-8-ANEPPS, 488 nm for MitoTracker, and 543 nm for Φ-O-Me-cAMP. Emission was at λ_{em} >670 nm for di-8-ANEPPS, 500<λ_{em} < 550 for MitoTracker and 595<λ_{em} < 625 for Φ-O-Me-CAMP.

ACKNOWLEDGMENTS. We thank Mikael Habtezion, Michael Kim, and Khanah Dao for technical assistance. This work was supported by American Heart Association Postdoctoral Fellowship 13POST14500067 (to L.P.), National Institutes of Health Grants P01-HL80101 and R37-HL030077 (to D.M.B.), and Fondation LeDucq (08CVD01).

1. Beavo JA, Brunton LL (2002) Cyclic nucleotide research—still expanding after half a century. *Nat Rev Mol Cell Biol* 3(9):710–718.
2. de Rooij J, et al. (1998) Epac is a Rap1 guanine-nucleotide-exchange factor directly activated by cyclic AMP. *Nature* 396(6710):474–477.
3. Kawasaki H, et al. (1998) A family of cAMP-binding proteins that directly activate Rap1. *Science* 282(5397):2275–2279.
4. Hothi SS, et al. (2008) Epac activation, altered calcium homeostasis and ventricular arrhythmogenesis in the murine heart. *Pflugers Arch* 457(2):253–270.
5. Métrich M, et al. (2010) Epac activation induces histone deacetylase nuclear export via a Ras-dependent signalling pathway. *Cell Signal* 22(10):1459–1468.
6. Métrich M, et al. (2008) Epac mediates beta-adrenergic receptor-induced cardiomyocyte hypertrophy. *Circ Res* 102(8):959–965.
7. Morel E, et al. (2005) cAMP-binding protein Epac induces cardiomyocyte hypertrophy. *Circ Res* 97(12):1296–1304.
8. Oestreich EA, et al. (2009) Epac and phospholipase Cepsilon regulate Ca^{2+} release in the heart by activation of protein kinase Cepsilon and calcium-calmodulin kinase II. *J Biol Chem* 284(3):1514–1522.
9. Oestreich EA, et al. (2007) Epac-mediated activation of phospholipase C(epsilon) plays a critical role in beta-adrenergic receptor-dependent enhancement of Ca^{2+} mobilization in cardiac myocytes. *J Biol Chem* 282(8):5488–5495.
10. Pereira L, et al. (2007) The cAMP binding protein Epac modulates Ca^{2+} sparks by a Ca^{2+}/calmodulin kinase signalling pathway in rat cardiac myocytes. *J Physiol* 583(Pt 2):685–694.
11. Pereira L, et al. (2012) Epac enhances excitation-transcription coupling in cardiac myocytes. *J Mol Cell Cardiol* 52(1):283–291.
12. Ruiz-Hurtado G, et al. (2012) Sustained Epac activation induces calmodulin dependent positive inotropic effect in adult cardiomyocytes. *J Mol Cell Cardiol* 53(5):617–625.
13. Ulucan C, et al. (2007) Developmental changes in gene expression of Epac and its upregulation in myocardial hypertrophy. *Am J Physiol Heart Circ Physiol* 293(3):H1662–H1672.
14. Pereira L, et al. (2013) Epac2 mediates cardiac β1-adrenergic-dependent sarcoplasmic reticulum Ca2+ leak and arrhythmia. *Circulation* 127(8):913–922.
15. Gloerich M, Bos JL (2010) Epac: Defining a new mechanism for cAMP action. *Annu Rev Pharmacol Toxicol* 50:355–375.
16. Niimura M, et al. (2009) Critical role of the N-terminal cyclic AMP-binding domain of Epac2 in its subcellular localization and function. *J Cell Physiol* 219(3):652–658.
17. Borland G, et al. (2006) Microtubule-associated protein 1B-light chain 1 enhances activation of Rap1 by exchange protein activated by cyclic AMP but not intracellular targeting. *Mol Pharmacol* 69(1):374–384.
18. DiPilato LM, Cheng X, Zhang J (2004) Fluorescent indicators of cAMP and Epac activation reveal differential dynamics of cAMP signaling within discrete subcellular compartments. *Proc Natl Acad Sci USA* 101(47):16513–16518.
19. Hochbaum D, Hong K, Barila G, Ribeiro-Neto F, Altschuler DL (2008) Epac, in synergy with cAMP-dependent protein kinase (PKA), is required for cAMP-mediated mitogenesis. *J Biol Chem* 283(8):4464–4468.
20. Nikolaev VO, Bünemann M, Hein L, Hannawacker A, Lohse MJ (2004) Novel single chain cAMP sensors for receptor-induced signal propagation. *J Biol Chem* 279(36): 37215–37218.
21. Ponsioen B, et al. (2004) Detecting cAMP-induced Epac activation by fluorescence resonance energy transfer: Epac as a novel cAMP indicator. *EMBO Rep* 5(12):1176–1180.
22. Qiao J, Mei FC, Popov VL, Vergara LA, Cheng X (2002) Cell cycle-dependent subcellular localization of exchange factor directly activated by cAMP. *J Biol Chem* 277(29): 26581–26586.
23. Ponsioen B, et al. (2009) Direct spatial control of Epac1 by cyclic AMP. *Mol Cell Biol* 29(10):2521–2531.
24. Dodge-Kafka KL, et al. (2005) The protein kinase A anchoring protein mAKAP coordinates two integrated cAMP effector pathways. *Nature* 437(7058):574–578.
25. Kapiloff MS, Jackson N, Airhart N (2001) mAKAP and the ryanodine receptor are part of a multi-component signaling complex on the cardiomyocyte nuclear envelope. *J Cell Sci* 114(Pt 17):3167–3176.
26. Enserink JM, et al. (2002) A novel Epac-specific cAMP analogue demonstrates independent regulation of Rap1 and ERK. *Nat Cell Biol* 4(11):901–906.
27. Rehmann H, Schwede F, Døskeland SO, Wittinghofer A, Bos JL (2003) Ligand-mediated activation of the cAMP-responsive guanine nucleotide exchange factor Epac. *J Biol Chem* 278(40):38548–38556.
28. Christensen AE, et al. (2003) cAMP analog mapping of Epac1 and cAMP kinase. Discriminating analogs demonstrate that Epac and cAMP kinase act synergistically to promote PC-12 cell neurite extension. *J Biol Chem* 278(37):35394–35402.
29. Moll D, et al. (2008) Biochemical characterization and cellular imaging of a novel, membrane permeable fluorescent cAMP analog. *BMC Biochem* 9:18.
30. de Rooij J, et al. (2000) Mechanism of regulation of the Epac family of cAMP-dependent RapGEFs. *J Biol Chem* 275(27):20829–20836.
31. Erickson JR, Patel R, Ferguson A, Bossuyt J, Bers DM (2011) Fluorescence resonance energy transfer-based sensor Camui provides new insight into mechanisms of calcium/calmodulin-dependent protein kinase II activation in intact cardiomyocytes. *Circ Res* 109(7):729–738.
32. Wu X, et al. (2006) Local InsP3-dependent perinuclear Ca^{2+} signaling in cardiac myocyte excitation-transcription coupling. *J Clin Invest* 116(3):675–682.
33. Holz GG, Chepurny OG, Schwede F (2008) Epac-selective cAMP analogs: New tools with which to evaluate the signal transduction properties of cAMP-regulated guanine nucleotide exchange factors. *Cell Signal* 20(1):10–20.
34. Vliem MJ, et al. (2008) 8-pCPT-2′-O-Me-cAMP-AM: An improved Epac-selective cAMP analogue. *ChemBioChem* 9(13):2052–2054.
35. Shaner NC, Steinbach PA, Tsien RY (2005) A guide to choosing fluorescent proteins. *Nat Methods* 2(12):905–909.
36. Cheng X, Ji Z, Tsalkova T, Mei F (2008) Epac and PKA: A tale of two intracellular cAMP receptors. *Acta Biochim Biophys Sin (Shanghai)* 40(7):651–662.
37. Laxman S, Riechers A, Sadilek M, Schwede F, Beavo JA (2006) Hydrolysis products of cAMP analogs cause transformation of Trypanosoma brucei from slender to stumpy-like forms. *Proc Natl Acad Sci USA* 103(50):19194–19199.
38. Fabiato A, Fabiato F (1979) Use of chlorotetracycline fluorescence to demonstrate Ca^{2+}-induced release of Ca^{2+} from the sarcoplasmic reticulum of skinned cardiac cells. *Nature* 281(5727):146–148.
39. Fabiato A, Fabiato F (1979) Calcium and cardiac excitation-contraction coupling. *Annu Rev Physiol* 41:473–484.
40. Aflaki M, et al. (2014) Exchange protein directly activated by cAMP mediates slow delayed-rectifier current remodeling by sustained β-adrenergic activation in guinea pig hearts. *Circ Res* 114(6):993–1003.
41. Brette F, Blandin E, Simard C, Guinamard R, Sallé L (2013) Epac activator critically regulates action potential duration by decreasing potassium current in rat adult ventricle. *J Mol Cell Cardiol* 57:96–105.
42. Mangmool S, Shukla AK, Rockman HA (2010) beta-Arrestin-dependent activation of $Ca^{(2+)}$/calmodulin kinase II after beta(1)-adrenergic receptor stimulation. *J Cell Biol* 189(3):573–587.